Study of Small Water Clusters Using the Effective Fragment Potential Model

Grant N. Merrill and Mark S. Gordon*

Department of Chemistry, Iowa State University, Ames, Iowa 50011

Received: October 16, 1997; In Final Form: January 5, 1998

The recently developed effective fragment potential (EFP) model is applied to the description of a series of small water clusters, $(H_2O)_n$, $n = 3-5$. These results are compared with those found in the literature. The model accurately reproduces results obtained at ab initio levels of theory, while the computational cost is comparable to that of models employing empirical potentials. The EFP model thus offers significant promise as an inexpensive alternative to the Hartree−Fock methodology in the treatment of small water clusters.

Introduction

The development of models that accurately describe the chemistry of condensed phases continues to be an active area of research in theoretical chemistry. The fact that no single methodology has met with universal acceptance offers powerful testament to the complexity surrounding solvation phenomena. While the sheer number of proposed models has proliferated over the past two decades, most are variations on two general themes.

By far, the most popular approach relies upon some implementation of the Onsager reaction field model,[1] where the bulk polarizability of the solvent couples with the electric field of the solute via a modified Hamiltonian. The behavior of these continuum-type models[2] is ultimately governed by the solvent's dielectric constant and the shape of the cavity that encloses the solute. While the sophistication of this type of model has steadily grown (e.g., the use of multipolar expansions beyond the dipole term and nonspherical cavities), they all suffer from the same inherent limitation: the inability to take account of specific intermolecular (e.g., solute−solvent and solvent−solvent) interactions. It is this shortcoming that frequently precludes physically meaningful insights into many of the important types of intermolecular phenomena (e.g., hydrogen bonding).

As a result of this limitation, models that explicitly consider solute−solvent and solvent−solvent interactions have been developed. These discrete models[3] constitute the second principal approach to problems associated with solvation. At the heart of these models lie various potentials for describing the specific interactions. These potentials range from the entirely empirical (e.g., TIP4P) to the fully quantum mechanical, the tradeoff being one of cost versus accuracy. While empirical potentials, owing to their simplicity, have become the mainstay of the simulation community, it has become increasingly apparent that they possess limited ability to reproduce ab initio calculations, particularly small-to-moderate sized clusters of solvent molecules (vide infra). This observation suggests that more accurate potentials are needed that are capable of describing both bulk behavior and specific intermolecular interactions.

Very recently, Wales and Walsh[4] have published several papers on the structures, relative energies, and isomerization reaction paths for a number of small water clusters. One focus of their studies was the comparison of Hartree−Fock (HF) ab initio calculations with several model potentials. The performance of these model potentials was found to be somewhat disappointing since they exhibited different conformational topologies, especially for the tetramers and pentamers. This is not entirely surprising as these empirical potentials are fit to reproduce bulk behavior. Nonetheless, the ultimate goal of any theoretical treatment of solvation should be a model that is capable of reproducing the characteristics of both clusters and bulk.

We have recently introduced an ab initio potential[5] (briefly outlined in the next section) that attempts to address many of the concerns surrounding purely empirical potentials. Moreover, calculations that make use of this potential will be shown to be only slightly more expensive than their empirical counterparts.

This paper offers a critical assessment of our "effective fragment potential" (EFP) via application to the potential energy surfaces of small water clusters, $(H_2O)_n$, $n = 3-5$. Whenever possible, the results are compared with those obtained from more conventional approaches, i.e., gas-phase ab initio and empirical potentials. Small water clusters offer a particularly compelling test of any potential as these systems may be viewed as a first approximation to bulk behavior.

Theoretical Methods

Only a cursory description of the effective fragment potential (EFP) model will be given as a conceptual framework from within which the reader may interpret the current results. A more thorough discussion can be found in previous papers.[5b,c] The EFP scheme divides the system of interest into two regions, the "active" and the "spectator" regions:

$$H_{\mathrm{TOT}} = H_{\mathrm{AR}} + H_{\mathrm{SR}} \tag{1}$$

The active region (AR) contains the solute and any solvent molecules that directly participate in bond making or breaking processes. This region is treated with an ab initio Hamiltonian, H_{AR}.

The effective fragment potential arising from the spectator (fragment) solvent molecules (SR) is treated via three one-electron terms, each corresponding to a particular component of the total interaction: electrostatic, H_k^{ELEC}; polarization, H_l^{POL}; and exchange repulsion/charge transfer:

$$H_{\mathrm{SR}} = \sum_k^K H_k^{\mathrm{ELEC}} + \sum_l^L H_l^{\mathrm{POL}} + \sum_m^M H_m^{\mathrm{REP}} \tag{2}$$

S1089-5639(97)03363-X CCC: $15.00
Published on Web 03/28/1998

The sum in each term on the right-hand side of eq 2 runs over the fragment coordinates of the spectator region and includes interactions between each fragment and the electrons and nuclei of the active region. Of course, there is no exchange repulsion/charge-transfer interaction between the active region nuclei and the fragments.

The electrostatic potential, H_k^{ELEC}, is based upon a distributed multipolar[6] expansion at a series of points within the fragments. The expansion is carried out through the octupole term, and the expansion points are located at the atomic centers and bond midpoints ($K = 5$ in eq 2 for a water fragment). Given that the electrostatic potential is a point charge model, it is necessary to employ distance-dependent cutoff functions to account for overlapping electron densities.

The polarization potential, H_l^{POL}, was derived from a self-consistent perturbation model[7] in which bond and lone pair, localized orbital, dipole polarizabilities of the valence shell were employed. These polarizabilities were obtained from isolated fragment molecules and are situated at the centroids of the orbitals ($L = 4$ in eq 2 for a water fragment). Since each region (active and spectator) polarizes the other, this term is iterated to self-consistency.

By performing Hartree−Fock calculations at approximately 200 water dimer orientations, the energy due to exchange repulsion/charge transfer was calculated by subtracting the electrostatic and polarization energies from the total potential energy, E^{TOT}:

$$E^{\mathrm{REP}} = E^{\mathrm{TOT}} - (E^{\mathrm{ELEC}} + E^{\mathrm{POL}}) \qquad (3)$$

The potential itself, H_m^{REP}, was obtained from a fit of these energies to a linear combination of two Gaussian functions ($M = 2$ in eq 2) for the AR−SR (solute−fragment) interaction or to a single exponential function for the SR−SR (fragment−fragment) interaction.

The EFP model uses a rigid-body approximation; the internal coordinates of the fragments are fixed at their experimental values (OH bond = 0.944 Å and HOH angle = 106.7°), while the positions of the fragments relative to the solute or each other are fully optimized. The effective fragment potential (EFP) has been incorporated within the GAMESS[8] suite of programs. Since analytic gradients have been derived and implemented for the EFP model, the geometries and energetics associated with minima and transition states on solvated potential energy surfaces are accessible. Surface curvatures in the vicinity of stationary points can be determined from the calculation of corresponding Hessian (energy second derivative) matrixes. As the goal of this study was to test the effective fragment potential itself, the code has recently been modified to permit runs in the absence of an active region ($H_{\mathrm{TOT}} = H_{\mathrm{SR}}$). Therefore, unless otherwise noted, all of the following results pertain to fragment−fragment interactions only, i.e., the sums in eq 2 run simply over the fragment coordinates.

Results and Discussion

A large number of experimental and computational (molecular mechanics, semiempirical, and ab initio electronic structure calculations as well as molecular dynamics and Monte Carlo simulations) studies on small water clusters have been reported in the literature.[9] While an ab initio approach is clearly preferable to ensure a high degree of accuracy, the cost associated with this level of theory rapidly becomes prohibitive as the size of the water cluster grows. For instance, with a modest double-split-valence basis set with diffuse and polarization functions on all atoms (e.g., 6-31++G**), the largest system considered here, that of the water pentamer, already requires 155 basis functions.

Emphasis has, therefore, been placed upon the development of potentials, usually classical in nature, that are computationally inexpensive. Ab initio calculations have thus achieved their utility in the current context as a means of providing parameters for and assessing the quality of a given potential. Ab initio calculations from the systematic studies of Wales and Walsh will serve as benchmarks for results obtained with the effective fragment potential. The HF/DZP(+)[10] level of theory is reasonable in terms of cost and accuracy for evaluating the EFP model, which was developed at a similar theoretical level.

Trimer

Of all the small water clusters, only the dimer has received more attention than the trimer, $(H_2O)_3$, from experimental and theoretical chemists. Wales and Walsh[4a,c] have published results from computations carried out at a variety of levels of theory. Unless noted otherwise, their work at the HF/DZP+ level will serve as the reference in evaluating the EFP results.

The lowest energy isomers for the smaller water clusters ($n \leq 5$) are thought to be monocyclic with each water monomer participating as a single hydrogen-bond donor and acceptor. Structures with multiple rings and those with monomers acting as double hydrogen-bond donors or acceptors have been found to be higher in energy. This is because it is energetically favorable to maximize the number of O···HO hydrogen bonds while minimizing their deviation from an ideal linear orientation.

Schütz and co-workers[11] have offered a nomenclature for these cyclic structures based upon whether the hydrogen atom of the donor monomer that is not participating in the intermolecular bond is above (up, "u"), below (down, "d"), or in the plane of (planar, "p") the ring. There is also the additional possibility that the plane of the ring may bisect (bifurcate, "b") the HOH angle of the donor monomer. This nomenclature will be used for the water trimer and tetramer systems. The increased complexity of the pentamer will demand a somewhat different approach (vide infra).

The global minimum (**1**) on the trimer potential energy surface is predicted by the effective fragment potential to have two of the nonbonding hydrogen atoms above and one below the ring plane, i.e., (uud). This result is consistent with those obtained at the HF/DZP+ level and with the TIP4P potential.[4a,c] The (uud) minimum is illustrated in Figure 1. A comparison with the HF structure reveals that hydrogen bonds are overestimated on average by 0.033 Å (standard deviation, $\sigma = 0.006$ Å) by the EFP model. This tendency by the EFP model to yield hydrogen bonds that are slightly longer than those calculated at the Hartree−Fock level has been noted earlier[5c] and was consistently found for the water trimers, tetramers, and pentamers.

The structural similarities for the two methods (ab initio and EFP) are also evident from the rotational constants determined for the (uud) minimum (Table 1). The values computed with the effective fragment potential are on average 0.002 GHz ($\sigma = 0.025$ GHz) lower than those found at the Hartree−Fock level. This small difference is consistent with the fact that there is only a slightly greater separation between the monomers in the EFP structure. A comparison with experiment for the (uud) minimum reveals both the HF and EFP values to be in good agreement.[12]

Wales and Walsh[4a,c] have reported the existence of two transition states (**2**−**3**) that correspond to degenerate rearrange-

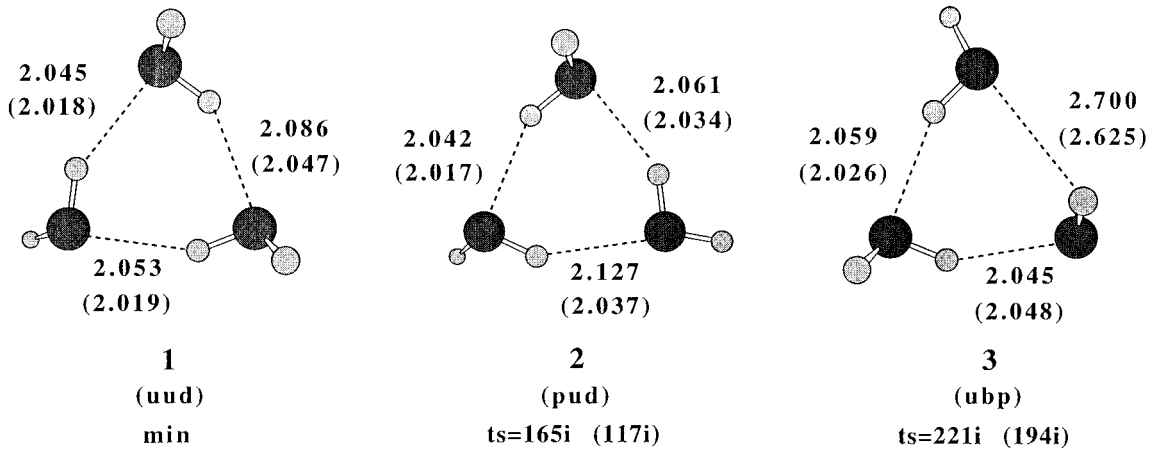

Figure 1. Water trimer, $(H_2O)_3$, minimum (min), and transition state (ts) structures obtained with the effective fragment potential (EFP). Parenthetical values are for the HF/DZP+ level of theory.[4a,c] Bond distances are given in angstroms (Å) and frequencies in wavenumbers (cm^{-1}).

TABLE 1: Rotational Constants *A*, *B*, and *C* (GHz) for Minimum-Energy Water Trimer, Tetramer, and Pentamer Structures[a]

	HF/DZP(+)[b]			EFP		
structure	A	B	C	A	B	C
(uud)[c] **1**	6.412 (6.647)	6.316	3.217 (3.324)[f]	6.425	6.285	3.228
(udud)[d] **4**	3.311 (3.080)	3.311	1.687 (1.540)[f]	3.323	3.315	1.692
(uudd) **5**	3.310	3.271	1.658	3.312	3.269	1.663
cyclic[e] **9**	1.895 (1.751)	1.892	0.966 (0.876)[f]	1.858	1.851	0.945
sqtr1 **10**	2.575	1.586	1.145	2.587	1.543	1.132
sqtr2 **11**	2.562	1.603	1.168	2.586	1.554	1.144
ebtet1 **12**	2.347	1.838	1.617	2.344	1.816	1.617
tbp **13**	2.097	1.816	1.774	2.088	1.798	1.777
ebtet2 **14**	2.343	1.846	1.603	2.360	1.814	1.590
sqtr3 **15**	2.509	1.575	1.247	2.593	1.706	1.500
sqtr4 **16**	2.531	1.546	1.207	2.470	1.575	1.236
sqtr5 **17**	2.387	1.634	1.297	2.394	1.625	1.285
sqtm1 **18**	2.750	1.148	0.905	2.708	1.139	0.902
sqtm2 **19**	2.856	1.089	0.863	2.784	1.093	0.871

[a] HF/DZP(+) results are those of Wales and Walsh.[4] Parenthetical values are from experiment. [b] The following basis sets were used: **1**, **4**, and **5**, DZP+; **9**−**19**, DZP. [c] Reference 12. [d] For $(D_2O)_4$; see ref 13. [e] For $(D_2O)_5$; see ref 19. [f] Assumes a planar, oblate top (i.e., $A = B \neq 2C$ and $C \sim 2A$).

TABLE 2: Relative Energies (kcal/mol) of Stationary Points on the Water Trimer, $(H_2O)_3$, Potential Energy Surface[a]

structure	HF/DZP+	EFP	TIP4P
(uud) **1**	0.00	0.00	0.00
(pud) **2**	0.07 (117*i*)	0.25 (165*i*)	0.02
(ubp) **3**	1.66 (194*i*)	1.72 (221*i*)	3.06

[a] Parenthetical values are frequencies in wavenumbers (cm^{-1}). HF/DZP+ and TIP4P results are those of Wales and Walsh.[4a,c]

ments of the (uud) minima. The (pud) transition state is predicted by the effective fragment potential to lie only 0.25 kcal/mol higher in energy than the (uud) minimum (Table 2). Calculations at the Hartree−Fock level[4a,c] and with the TIP4P potential[4a,c] predict that this transition state is essentially degenerate with that of the global minimum. The (pud) transition state corresponds to the flipping of one of the "up" hydrogen atoms in the (uud) minimum. The associated vibrational frequency (165*i* cm^{-1}) is indicative of a loose transition state and is in good agreement with the HF/DZP+ value of 117*i* cm^{-1}.

The (ubp) transition state lies somewhat higher in energy than the other trimer stationary points. The energies relative to the (uud) minimum determined from the EFP (1.72 kcal/mol) and Hartree−Fock (1.66 kcal/mol) calculations are in good agreement with one another, while the TIP4P value (3.06 kcal/mol)[4a,c] is nearly double that found at the ab initio level.[4a,c] This transition state involves a concerted but asynchronous process of rotation of one monomer about its C_2 axis and inversion of a nonbonding hydrogen atom in a second monomer. Therefore, the associated force constant is larger in magnitude than that found for the previous transition state, as evidenced by vibrational frequencies of 221*i* (EFP) and 194*i* (HF/DZP+) cm^{-1}.

An examination of the hydrogen bonding in the two transition-state structures shows that the agreement between the Hartree−Fock and EFP calculations is nearly as good as that found for the minima. The effective fragment potential leads to intermolecular bonds that are on average 0.041 Å ($\sigma = 0.034$ Å) longer than those predicted at the Hartree−Fock level.

Tetramer

Wales and Walsh[4d] have recently completed a computational survey of the water tetramer, $(H_2O)_4$, potential energy surface. The study includes results obtained at the Hartree−Fock level (HF/DZP+) as well as those from an empirical potential (ASP−W2).

The water tetramer structures are illustrated in Figure 2. Analogous to the results obtained for the water trimer, the two lowest energy minima (**4**−**5**) located with the effective fragment potential possess monocyclic geometries. The structure in which the free hydrogen atoms alternate above and below the plane of the ring, (udud), is predicted to be 0.86 kcal/mol (Table 3) lower in energy than that of the structure with two eclipsing interactions, (uudd). This relative ordering of energies reproduces precisely those found at the Hartree−Fock level. The ASP−W2 potential leads to an energy difference between the two minima that is slightly smaller. In addition, the ASP−W2 potential predicts minima on the surface that are not found by the other two methods.[4d] Hydrogen bond distances determined with the effective fragment potential are on average 0.012 Å ($\sigma = 0.004$ Å) longer than those found for the ab initio structures.

Table 1 lists rotational constants calculated at the HF/DZP+ level and with the effective fragment potential for the two water tetramer minima. A comparison between the two sets of data shows that the EFP model overestimates the Hartree−Fock rotational constants on average by 0.004 GHz ($\sigma = 0.005$ GHz). The close similarity of these values offers further evidence that the effective fragment potential is capable of reproducing Hartree−Fock structures. For the (udud) minimum, experi-

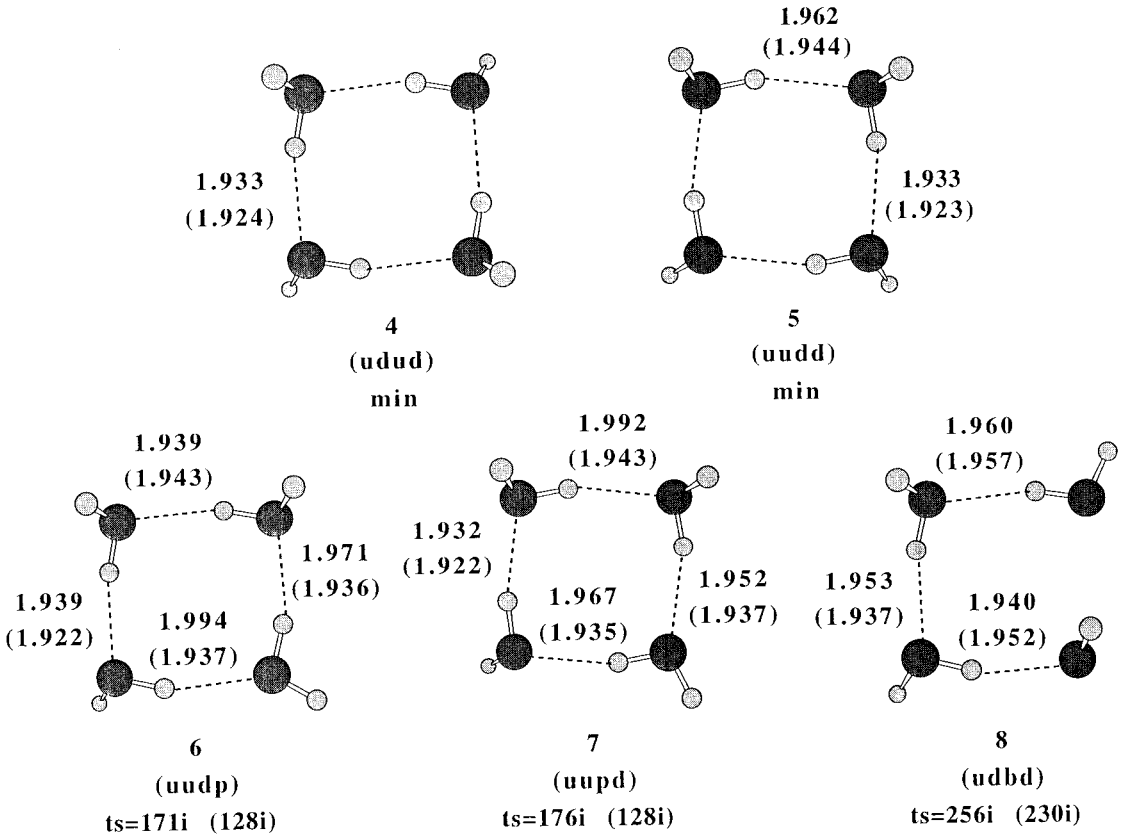

Figure 2. Water tetramer, $(H_2O)_4$, minimum (min), and transition state (ts) structures obtained with the effective fragment potential (EFP). Parenthetical values are for the HF/DZP+ level of theory.[4d] Bond distances are given in angstroms (Å) and frequencies in wavenumbers (cm^{-1}).

TABLE 3: Relative Energies (kcal/mol) of Stationary Points on the Water Tetramer $(H_2O)_4$ Potential Energy Surface[a]

structure	HF/DZP+	EFP	ASP−W2
(udud) **4**	0.00	0.00	0.00
(uudd) **5**	0.85	0.86	0.75
(uudp) **6**	0.93 (128*i*)	1.18 (171*i*)	1.47
(uupd) **7**	0.94 (128*i*)	1.18 (176*i*)	1.46
(udbd) **8**	2.55 (230*i*)	2.56 (256*i*)	1.68

[a] Parenthetical values are frequencies in wavenumbers (cm^{-1}). HF/DZP+ and ASP-W2 results are those of Walsh and Wales.[4d]

mental rotation constants have been determined for the $(D_2O)_4$ isotopomer.[13] Once again, both the EFP and HF values are in fairly good agreement with those of experiment, the latter being slightly smaller due to the greater mass of the perdeuterated monomers.

Three transition states (**6**−**8**) related to the above two minima were identified with both HF/DZP+ and the effective fragment potential. The two lower energy transition states, (uudp) and (uupd), interconvert the (udud) and (uudd) minima. As shown in Table 3, the EFP model predicts both to be 1.18 kcal/mol higher in energy than the global minimum, (udud). This results in only a 0.32 kcal/mol barrier relative to the (uudd) minimum. The ab initio transition states lie about 0.25 kcal/mol lower in energy. Both levels of theory predict that the two transition states may be characterized as "loose" (see Table 3); those determined at the Hartree−Fock level have imaginary vibrational frequencies that are about 25% smaller than the corresponding EFP values. Results obtained with the ASP−W2 potential are similar, except that the two transition states are about 0.30 kcal/mol higher in energy.

The third transition state, (udbd), is calculated to be higher in energy at both the HF/DZP+ level and with the EFP model. Both values are in excellent quantitative agreement with one another. The ASP−W2 potential leads to an energy that is 0.87 kcal/mol lower than that found at the HF/DZP+ level; this value is also much closer to the other two transition states. The imaginary frequencies associated with the (udbd) transition state are also higher by 82*i* (EFP) and 59*i* (HF/DZP+) cm^{-1}, so this (udbd) transition state is somewhat tighter than those of the (uudp) or (uupd) structures. A comparison of the geometries (Figure 2) reveals that, as with the minima, the EFP method tends to predict hydrogen bond distances that are slightly elongated (on average 0.020 Å; $\sigma = 0.021$ Å) relative to the HF values.

One discrepancy between the effective fragment and ab initio potential energy surfaces centers around the (udbd) transition state. While the Hartree−Fock transition state of Wales and Walsh is reported to connect two identical (udud) minima, the EFP model predicts that it corresponds to the conversion of the (udud) and (uudd) minima and is thus similar to the (uudp) and (uupd) transition states. Whereas Wales and Walsh[4d] employed an eigenvector-following (EF)[14] routine to establish which minima correspond to a given transition state, the present work made use of an intrinsic reaction coordinate (IRC)[15] method. The two approaches are not strictly equivalent. The IRC technique calculates a minimum energy path between reactants and products via a given transition state. The EF method does not guarantee that the minimum energy path is followed upon displacement from the same transition state. This difference offers a possible explanation for the prediction that different reaction paths were obtained from nominally the same transition state. Such differences are expected to occur most frequently for potential energy surfaces that (1) are relatively flat, like those associated with small water clusters, where barriers separating neighboring minima are often very small and/or (2) possess a great many minima and transition states that lie close in energy.

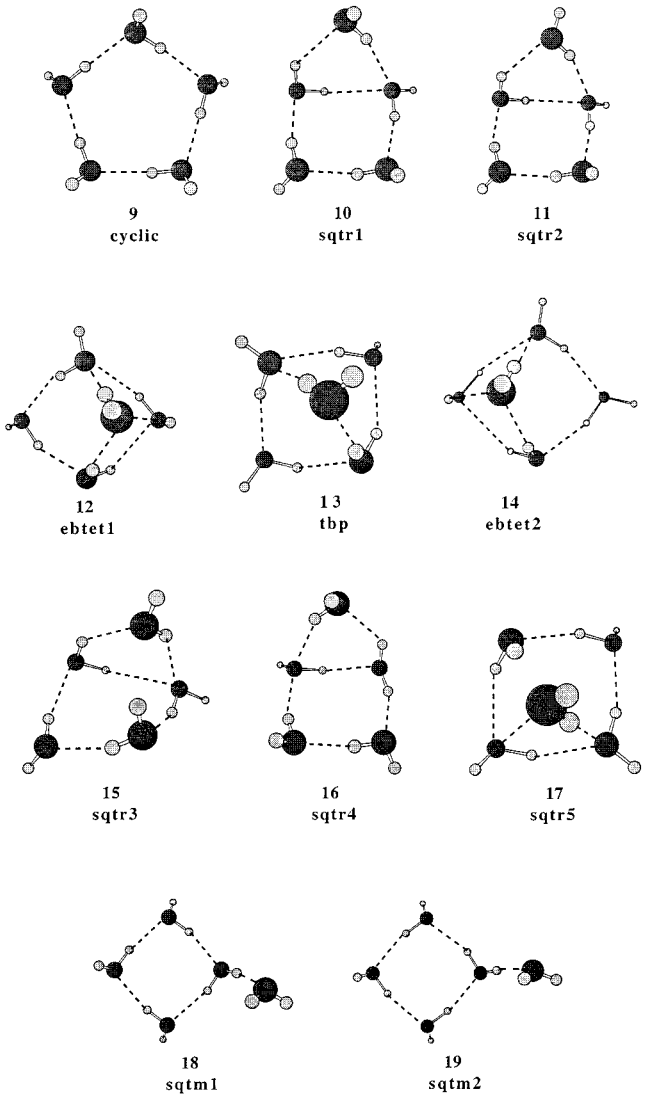

Figure 3. Water pentamer, $(H_2O)_5$, minimum energy structures obtained with the effective fragment potential (EFP).

The foregoing hypothesis was confirmed by determining the HF/DH**++[16] (udbd) transition state and the corresponding minimum-energy path from an IRC calculation. This ab initio IRC was found to be consistent with that determined with the effective fragment potential, i.e., the (udbd) transition state connects the (udud) and (uudd) minima.

Given the extremely flat nature of all the water cluster potential energy surfaces, systems with nonzero thermodynamic temperatures will not follow minimum-energy paths closely.[17] Crossing and recrossing between the various reactant and product channels is not only possible but probable.

Pentamer

Eleven HF/DZP water pentamer minima were located by Wales and Walsh.[4b] These are reproduced in Figure 3. Given the increased complexity of the system, a new nomenclature[4b] was adopted to describe the water pentamers: "cyclic", a single, five-membered ring (**9**); "sqtr", *square-triangle* in which the edge of a four-membered ring is bridged by the fifth water molecule (**10**−**11**, **15**−**17**); "sqtm", *square-terminal* where the fifth water molecule is hydrogen bonded to only one molecule of the four-membered ring (**18**−**19**); "ebtet", *edged-bridged tetrahedron* (**12**, **14**); and "tbp", *trigonal bipyramid* (**13**).

TABLE 4: Relative Energies (kcal/mol) of Minima on the Water Pentamer, $(H_2O)_5$, Potential Energy Surface[a]

structure[b]	HF/DZP	EFP	structure	HF/DZP	EFP
cyclic **9**	0.00	0.00	sqtr3 **15**	3.11	1.49
sqtr1 **10**	1.55	0.86	sqtr4 **16**	3.15	2.46
sqtr2 **11**	1.57	0.90	sqtr5 **17**	3.45	2.78
ebtet1 **12**	2.17	1.21	sqtm1 **18**	3.80	3.22
tbp **13**	2.21	1.20	sqtm2 **19**	3.87	3.28
ebtet2 **14**	2.35	1.44			

[a] HF/DZP results are those of Wales and Walsh.[4b] [b] The structures themselves are illustrated in Figure 3.

The HF and EFP relative energies of these 11 minima are given in Table 4. Both sets of calculations predict that the lowest energy structure is the cyclic species and all of the energies cover a narrow range (3.87 and 3.28 kcal/mol for the HF and EFP methods, respectively). While the effective fragment potential essentially reproduces the relative ordering of energies at the Hartree−Fock level, they are on average 0.84 kcal/mol lower.[18] The worst agreement is for the sqtr3 minimum where the EFP model underestimates the HF/DZP value by 1.62 kcal/mol.

As was the case for the water trimers and tetramers, the EFP pentamer bonds are on average 0.016 Å ($\sigma = 0.039$ Å) too long. Rotational constants calculated with the effective fragment potential (Table 1) closely approximate those determined at the Hartree−Fock level, yielding a mean difference of only 0.002 GHz ($\sigma = 0.059$ GHz). Saykally and co-workers[19] have recently determined rotational constants for the $(D_2O)_5$ cyclic isotopomer. The agreement between the experimental and computational values is similar to that found in the tetramer case.

Wales and Walsh[4b] have reported 14 transition states associated with the above eleven minima. They have been labeled here according to which minima they reportedly connect (e.g., "cyclic-sqtr2"). Hartree−Fock and effective fragment potential energies relative to the global minimum (cyclic) are listed in Table 5. The EFP model, once again, reproduces the relative ordering determined at the HF level; the EFP values are on average about 0.71 kcal/mol lower in energy. Two of the transition states (sqtr2−sqtr3 and tbp−sqtr1) were not located with the EFP model. The EFP transition state geometries have hydrogen bonds that are on average 0.028 Å longer ($\sigma = 0.040$ Å) than their ab initio analogues.

Minimum-energy paths leading away from these transition states were also computed for the effective fragment potential via the IRC method. For 6 of the 12 transition states (**20**−**23**, **29**, **32**), the associated minima were similar to those reported by Wales and Walsh.[4b] In the remaining six cases, new minima were discovered (Figure 4 and Table 6). HF/DH**++ calculations were once again carried out to ascertain the source of these discrepancies. IRC calculations for two of the transition states (**31**, **33**) led to minima that were consistent with those determined with the effective fragment potential and different from those found at the HF/DZP level via the EF method. For the other four transition states (**24**, **27**−**28**, **30**), the two sets of ab initio computations were in agreement with one another, i.e., the IRC (HF/DH**++) and EF (HF/DZP) calculations yield the same minima for these four transition states. Optimizations at the HF/DH**++ level of the four new EFP minima (**34**−**37**) led to previously identified structures. These results lead to the conclusion that the effective fragment and Hartree−Fock potentials, while quite similar, are not identical.

Wales and Walsh[4b] reexamined all of the above 14 reaction pathways with four different empirical potentials (TIP4P,[20] EPEN,[21] ASP−W2,[22] and ASP−W4[22]). As reported in their

TABLE 5: Relative Energies (kcal/mol) of Transition States on the Water Pentamer, $(H_2O)_5$, Potential Energy Surface[a]

structure[b]	HF/DZP	EFP	structure	HF/DZP	EFP
cyclic−cyclic 2 **20**	0.03 (71*i*)	0.15 (141*i*)	sqtr1−sqtr1 **27**	3.46 (52*i*)	1.85 (30*i*)
sqtr2−sqtr1 **21**	1.62 (85*i*)	1.04 (130*i*)	tbp−sqtr4 **28**	3.47 (50*i*)	2.55 (53*i*)
sqtr2−cyclic **22**	1.75 (50*i*)	1.60 (47*i*)	tbp−sqtr5 **29**	3.89 (51*i*)	3.09 (57*i*)
cyclic−cyclic 1 **23**	2.19 (249*i*)	2.01 (240*i*)	sqtr3−sqtm2 **30**	4.15 (37*i*)	3.48 (35*i*)
ebtet2−sqtr1 **24**	2.49 (39*i*)	1.85 (46*i*)	cyclic−sqtr2 **31**	4.22 (124*i*)	3.48 (95*i*)
sqtr2−sqtr3 **25**	3.16 (33*i*)	N.A.	sqtr1−ebtet1 **32**	4.60 (112*i*)	3.57 (106*i*)
tbp−sqtr1 **26**	3.44 (48*i*)	N.A.	sqtr2−sqtr2 **33**	4.66 (36*i*)	3.39 (22*i*)

[a] The transition states are labeled according to which minima they connect (e.g., the "sqtr2−cyclic" TS connects the "sqtr2" and "cyclic" minima). Energies are relative to cyclic minimum. N.A. signifies transition state not located. Parenthetical values are frequencies in wavenumbers (cm^{-1}). HF/DZP results are those of Wales and Walsh.[4b] [b] The minimum energy structures connected by these transition states are illustrated in Figure 3.

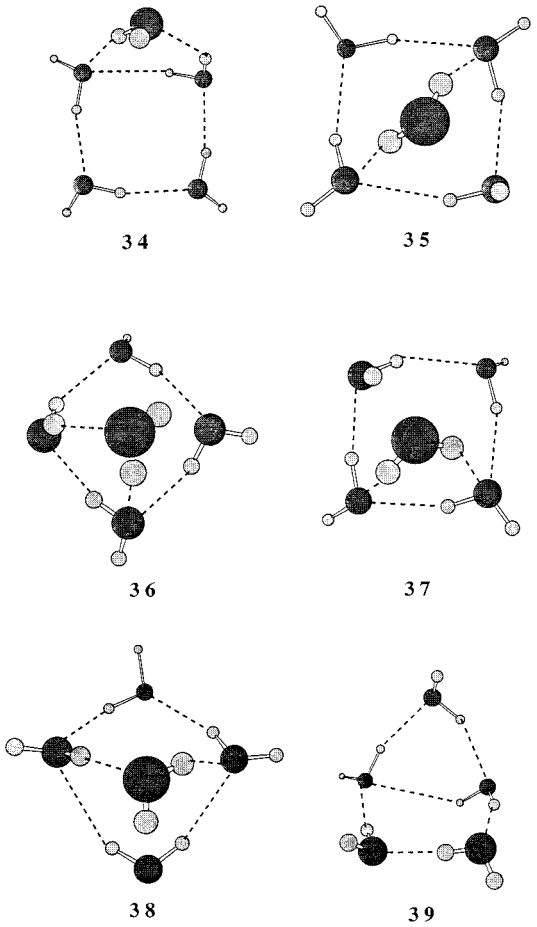

Figure 4. Novel water pentamer, $(H_2O)_5$, minimum energy structures obtained with the effective fragment potential (EFP) and HF/DH**++ level of theory.

study, "none of the empirical potentials were able to reproduce more than about four of the ab initio pathways, generally collapsing to ebtet-type structures instead" (p 6968, ref 4b). Their TIP4P results are representative of those obtained with the other potentials and will be briefly summarized in the next paragraph.

The TIP4P potential was capable of locating the two transition states associated with the degenerate rearrangement of the cyclic minimum: cyclic−cyclic 1 and cyclic−cyclic 2. The barrier for the former process was found to be 2.83 kcal/mol (HF/DZP = 2.19 kcal/mol; EFP = 2.01 kcal/mol), while the latter was determined to be essentially zero (HF/DZP = 0.03 kcal/mol; EFP = 0.15 kcal/mol). These results are consistent with earlier work by Tsai and Jordan.[23] In addition to these two degenerate isomerizations, Wales and Walsh reported that the ebtet2−sqtr1, sqtr2−cyclic, and cyclic−sqtr2 reactions paths were "also

TABLE 6: Relative Energies (kcal/mol) of Novel Water Pentamer, $(H_2O)_5$, Minima Found with the Effective Fragment Potential (EFP) and at the HF/DH++ (HF) Level of Theory[a]**

minimum	transition state	EFP	HF[b]
34	ebtet2−sqtr1 **24**	1.45	
35	sqtr1−sqtr1 **27**	1.71	
36	tbp−sqtr4 **28**	1.90	
37	tbp−sqtr4 **28**	2.15	
38	sqtr3−sqtm2 **30**	1.49	
39	cyclic−sqtr2 **31**	1.65	1.59
38	sqtr2−sqtr2 **33**	1.49	2.43

[a] All energies are relative to the cyclic minimum. [b] Blank entry indicates a minimum energy structure was not found.

TABLE 7: Many-Body Effects in $(H_2O)_n$, $n = 3-5$, Clusters (All Bond Distances are Averages and in Angstroms (Å))

parameter	trimer (uud)	tetramer (udud)	pentamer (cyclic)
r_{H-O} (EFP)	2.061	1.933	1.913
r_{H-O} (HF)	2.028	1.924	1.871
r_{O-O} (EFP)	2.902	2.855	2.853
r_{O-O} (HF)	2.897	2.856	2.824
r_{O-O} (expt)[a]	2.879	2.807	2.756

[a] Tetramer and pentamer are perdeuterated species; see ref 19.

qualitatively represented by the potential [TIP4P]" (p 6968, ref 4b), although no energetic data (i.e., barrier heights) were given.

It should be noted that while the authors conclude "the ASP potentials appear to give a reasonable account of the two most important mechanisms [cyclic−cyclic 1 and cyclic−cyclic 2]" (p 6969, ref 4b), both potentials do not predict the cyclic structure to be the global minimum. Of the four empirical potentials examined, EPEN performed the most poorly in reproducing the ab initio (HF/DZP) potential energy surface, failing to locate the cyclic and any of the "sqtr" minima.

As has been pointed out by Xantheas,[24] many-body or cooperative effects can contribute significantly to the stabilization energies of small water clusters. These effects should lead to a shortening of hydrogen bonds with an increase in the number of water monomers. Calculations at both the Hartree−Fock level and with the EFP model are consistent with these predictions (Table 7), where 92.8% (EFP) and 92.3% (HF) decreases in the average hydrogen bond length occur in going from the (uud) trimer to the cyclic pentamer. Similar, but less dramatic, changes are seen for average r_{O-O} bond distances. Both sets of calculations appear to be converging upon the ordered bulk value (r_{O-O} = 2.84 Å at 277 K).[25] These geometrical changes are also observed experimentally for the $(D_2O)_n$, $n = 3-5$, clusters.[19]

Timings

Table 8 lists the total CPU times required to calculate a single-point energy and gradient (the fundamental steps in a structural

TABLE 8: Total CPU Times (Seconds Unless Otherwise Noted) To Calculate a Single-Point Energy and Gradient for a Series of Water Clusters, $(H_2O)_n$, $n = 2-10$[a]

no. of monomers	TIP3P	EFP	AM1	HF/DZP[b]
2	0.4	0.5	0.7	61.8
3	0.5	0.5	0.9	271.8
4	0.5	0.7	1.1	787.9
5	0.6	0.9	1.4	1123.8
6	0.7	0.9	1.7	1405.5
7	0.7	1.2	2.2	1834.4
8	0.9	1.4	2.8	2714.4
9	1.0	1.9	3.2	3951.0
10	1.0	2.1	3.9	5476.7
100[c]	8.2	20.4	39.4	16.8 h
1000[c]	1.3 min	3.4 min	6.6 min	7.2 day

[a] All runs performed on an IBM RS/6000 Model 350 workstation. [b] Basis set has 25 functions per monomer. [c] Projected timings extrapolated from data on $(H_2O)_n$, $n = 2-10$. See ref 19 for specific equations.

optimization) at a variety of theoretical levels for a series of water clusters of increasing size. The geometries for these clusters were chosen randomly. All of the timings were obtained on an IBM RS/6000 Model 350 workstation. The least expensive set of computations employed the empirical TIP3P potential.[26] For the water decamer, only 1.0 s of CPU time was required to calculate a single-point energy and gradient. Extrapolation of the TIP3P data in Table 8 to the cases of 100 and 1000 water monomers led to projected timings of 8.2 s and 1.3 min, respectively.[27] The computational cost associated with the more accurate effective fragment potential increased only marginally (e.g., $(H_2O)_{1000}$, 3.4 min), so this potential is not only feasible but quite competitive with those of simple empirical models.

As semiempirical methods offer an inexpensive alternative to ab initio theory, they have enjoyed some popularity in the development and implementation of solvation models.[28] Timings have, therefore, been included in Table 8 for the AM1 Hamiltonian. This method proves to be about twice as costly as the EFP method. Finally, the Hartree−Fock level of theory is much more expensive and, therefore, applicable only to relatively small water clusters.

Conclusions

The application of the effective fragment potential to the description of the potential energy surfaces of small water clusters, $(H_2O)_n$, $n = 3-5$, demonstrates that the method is in general capable of reproducing results obtained at the Hartree−Fock level. Specifically, the relative ordering of HF/DZP(+) energies for both minima and transition states is reproduced by the EFP model with a mean absolute deviation of only 0.64 kcal/mol. Structures obtained with the EFP potential also compare favorably to those determined at the ab initio level with a mean absolute deviation in hydrogen bond distances of 0.035 Å. Given that the computational expense associated with the EFP model is comparable to that of popular empirical potentials and more faithfully reproduces the Hartree−Fock potential energy surfaces, the current method offers great promise as an accurate and cost-effective approach to the description of small aqueous clusters. Moreover, the effective fragment potential is based upon a quantum mechanical wave function and is thus amenable to ready physical interpretation. It is at present unclear how well the effective fragment potential will reproduce the bulk behavior of solvents, and molecular dynamics simulations are currently being carried out, the results of which will be reported in due course.

Acknowledgment. The authors are most grateful to Prof. David Wales, whose papers inspired this work and who has graciously provided his data on water clusters. This work was supported by a grant from N.I.S.T.

References and Notes

(1) Onsager, L. *J. Am. Chem. Soc.* **1936**, *58*, 1486.

(2) An excellent review of continuum methodologies may be found in: (a) Cramer, C. J.; Truhlar, D. G. *Reviews in Computational Chemistry*; Boyd, D. B., Lipkowitz, K. B., Eds.; VCH: New York, 1995; Vol. 6. For other examples of continuum solvation models, see: (b) Szafran, M.; Karelson, M. M.; Katritzky, A. R.; Koput, J.; Zerner, M. C. *J. Comput. Chem.* **1993**, *14*, 371. (c) Giesen, D. J.; Cramer, C. J.; Truhlar, D. G. *J. Phys. Chem.* **1995**, *99*, 7137. (d) Bianco, R.; Hynes, J. T. *J. Chem. Phys.* **1995**, *102*, 7864. (e) Tortonda, F. R.; Pascual-Ahuir, J.-L.; Silla, E.; Tunon, I. *J. Phys. Chem.* **1995**, *99*, 12525. (f) Truong, T. N.; Stepanovich, E. V. *J. Chem. Phys.* **1995**, *103*, 3709. (g) Giesen, D. J.; Storer, J. W.; Cramer, C. J.; Truhlar, D. G. *J. Am. Chem. Soc.* **1995**, *117*, 1057.

(3) For examples of discrete solvation models, see: (a) Warshel, A. *J. Phys. Chem.* **1979**, *83*, 1640. (b) Thole, B. T.; van Duijnen, P. T. *Theor. Chim. Acta* **1980**, *55*, 307. (c) Thole, B. T.; van Duijnen, P. T. *Chem. Phys.* **1982**, *71*, 211. (d) Singh, U. C.; Kollman, P. A. *J. Comput. Chem.* **1984**, *5*, 129. (e) Warshel, A.; King, G. *Chem. Phys. Lett.* **1985**, *121*, 124. (f) King, G.; Warshel, A. *J. Chem. Phys.* **1989**, *91*, 3647. (g) Field, M. J.; Bash, P. A.; Karplus, M. J. *J. Comput. Chem.* **1990**, *11*, 700. (h) Luzhkov, V.; Warshel, A. *J. Am. Chem. Soc.* **1991**, *113*, 4491. (i) Gao, J. *J. Am. Chem. Soc.* **1994**, *116*, 1563. (j) Thompson, M. A.; Glendening, E. D.; Feller, D. F. *J. Phys. Chem.* **1994**, *98*, 10465. (k) Maseras, F.; Morokuma, K. *J. Comput. Chem.* **1995**, *16*, 1170. (l) Gao, J. *J. Phys. Chem.* **1992**, *96*, 537. (m) Liu, H.; Müller-Plathe, F.; van Gunsteren, W. F. *J. Chem. Phys.* **1994**, *101*, 1722. (n) de Vries, A. H.; van Duijnen, P. T.; Juffer, A. H.; Rullman, A. C.; Dijkman, J. P.; Merenga, H.; Thole, B. T. *J. Comput. Chem.* **1995**, *16*, 37.

(4) (a) Wales, D. J. *J. Am. Chem. Soc.* **1993**, *115*, 11180. (b) Wales, D. J.; Walsh, T. R. *J. Chem. Phys.* **1996**, *105*, 6957. (c) Walsh, T. R.; Wales, D. J. *J. Chem. Soc., Faraday Trans.* **1996**, *92*, 2505. (d) Wales, D. J.; Walsh, T. R. *J. Chem. Phys.* **1997**, *106*, 7193. (e) Wales, D. J. *Advances in Molecular Vibrations and Collision Dynamics*, in press. (f) Wales, D. J. *Encyclopedia of Computational Chemistry*, in press.

(5) (a) Jensen, J. H.; Day, P. N.; Gordon, M. S.; Basch, H.; Cohen, D.; Garmer, D. R.; Krauss, M.; Stevens, W. J. *Modeling the Hydrogen Bond*; Smith, D. A., Ed.; ACS Symposium Series 569, 1994. (b) Day, P. N.; Jensen, J. H.; Gordon, M. S.; Webb, S. P.; Stevens, W. J.; Krauss, M.; Garmer, D.; Basch, H.; Cohen, D. *J. Chem. Phys.* **1996**, *105*, 1968. (c) Chen, W.; Gordon, M. S. *J. Chem. Phys.* **1996**, *105*, 11081. (d) Kraus, M.; Webb, S. P. *J. Chem. Phys.* **1997**, *107*, 5771. (e) Day, P. N.; Pachter, R. *J. Chem. Phys.* **1997**, *107*, 2990.

(6) (a) Stone, A. J. *Chem. Phys. Lett.* **1981**, *83*, 233. (b) Stone, A. J.; Alderton, M. *Mol. Phys.* **1985**, *56*, 1047.

(7) Garmer, D. R.; Stevens, W. J. *J. Phys. Chem.* **1989**, *93*, 8263.

(8) Schmidt, M. W.; Baldridge, K. K.; Boatz, J. A.; Jensen, J. H.; Koseki, S.; Matsunaga, N.; Gordon, M. S.; Ngugen, K. A.; Su, S.; Windus, T. L.; Elbert, S. T.; Montgomery, J.; Dupuis, M. *J. Comput. Chem.* **1993**, *14*, 1347.

(9) Comprehensive surveys of both experimental and computational results can be found in the articles of Wales and Walsh; see ref 4.

(10) Dunning, T. H. *J. Chem. Phys.* **1970**, *53*, 2823. The parentheses surrounding the symbol for diffuse functions, +, signifies that some of the Hartree−Fock calculations made use of basis sets that included diffuse s and sp functions on H and O atoms, respectively, while others did not. See text for details.

(11) Schütz, M.; Bürgi, T.; Leutwyler, S.; Bürgi, H. B. *J. Chem. Phys.* **1994**, *100*, 1780.

(12) Liu, K.; Loeser, J. G.; Elrod, M. J.; Host, B. C.; Rzepiela, J. A.; Pugliano, N.; Saykally, R. J. *J. Am. Chem. Soc.* **1994**, *116*, 3507.

(13) Cruzan, J. D.; Braly, L. B.; Liu, K.; Brown, M. G.; Loeser, J. G.; Saykally, R. J. *Science* **1996**, *271*, 59.

(14) (a) Hilderbrandt, R. L. *Comput. Chem.* **1977**, *1*, 179. (b) Baker, J. *J. Comput. Chem.* **1986**, *7*, 385.

(15) Gonsalez, C.; Schlegel, H. B. *J. Phys. Chem.* **1990**, *94*, 5523. Step sizes between 0.10 and 0.30 bohr·amu$^{1/2}$ were used. The final structures (minima) obtained from IRC runs were fully optimized and their associated Hessian matrixes calculated as a means of verifying that they were indeed minima.

(16) This basis set is nearly identical to that of ref 10: a double-ζ basis combined with sets of p and d polarization functions added to H and O atoms, respectively (Dunning, T. H.; Hay, P. J. *Methods of Electronic Structure Theory*; Schaefer, H. F., Ed.; Plenum Press: New York, 1977). Diffuse s and sp functions were also added to H and O atoms, respectively.

(17) In IRC calculations, the kinetic component of the total energy is set to zero at each step along the minimum-energy reaction path. The total energy of the system is, therefore, not conserved.

(18) Unlike their ab initio counterparts, all of the EFP values do not include zero-point energy (ZPE) corrections. These corrections have a negligible effect upon the relative energies. For example, the statistics for the water pentamer minima are representative: without ZPE, mean dissociation energy (DE) (EFP − HF/DZP) = −0.84 kcal/mol, standard deviation = 0.31 kcal/mol; with ZPE, mean DE = −0.87 kcal/mol, standard deviation = 0.31 kcal/mol.

(19) Liu, K.; Brown, M. G.; Cruzan, J. D.; Saykally, R. J. *Science* **1996**, *271*, 62. Bond lengths are based upon a fit of experimental r_{O-O} values; see Figure 3 of this reference.

(20) Jorgensen, W. L.; Chandrasekhar, J.; Madura, J. D.; Impey, R. W.; Klein, M. L. *J. Chem. Phys.* **1983**, *79*, 926.

(21) Owicki, J. C.; Shipman, L. L.; Scheraga, H. A. *J. Phys. Chem.* **1975**, *79*, 1794.

(22) Millot, C.; Stone, A. J. *Mol. Phys.* **1992**, *77*, 439.

(23) **.** Tsai, C. J.; Jordan, K. D. *J. Phys. Chem.* **1993**, *97*, 11227.

(24) Xantheas, S. S. *J. Chem. Phys.* **1994**, *100*, 7523.

(25) Narten, A. H.; Levy, H. A. *Water: A Comprehensive Treatise;* Franks, F., Ed.; Plenum: New York, 1972.

(26) The essential difference between the TIP3P and TIP4P potentials lies in the placement and magnitude of the monomer partial charges. See ref 17 for a complete description of the two potentials.

(27) Projected timings are based upon linear regressions determined from $(H_2O)_n$, $n = 2-10$. TIP3P: Y (time in sec) = 0.080 × X (number of monomers) + 0.220, $R^2 = 0.960$. EFP: $Y = 0.205 \times X - 0.108$, $R^2 = 0.935$. AM1: $Y = 0.398 \times X - 0.401$, $R^2 = 0.963$. HF/DZP: $Y = 621.010 \times X - 1767.5$, $R^2 = 0.899$. The assumption of linear scaling in these extrapolations is not strictly valid. For example, the TIP3P calculations actually scale as N^2, where N is the number of water monomers, and plots of N vs time should exhibit parabolic behavior. The degree of deviation from linearity may be seen in the R^2 values, i.e., the further an R^2 value is from unity, the less linear the relationship.

(28) Chambers, C. C.; Hawkins, G. D.; Cramer, C. J.; Truhlar, D. G. *J. Phys. Chem.* **1996**, *100*, 16385.